Proc. Natl. Acad. Sci. USA
Vol. 90, pp. 5076–5080, June 1993
Biochemistry

Three-dimensional structures of avidin and the avidin–biotin complex

(deglycosylated avidin/divergent evolution/x-ray crystallography/streptavidin)

ODED LIVNAH*, EDWARD A. BAYER†, MEIR WILCHEK†, AND JOEL L. SUSSMAN*

Departments of *Structural Biology and †Biophysics, The Weizmann Institute of Science, Rehovot 76100 Israel

Communicated by Christian B. Anfinsen, January 28, 1993 (received for review November 14, 1992)

ABSTRACT **The crystal structures of a deglycosylated form of the egg-white glycoprotein avidin and of its complex with biotin have been determined to 2.6 and 3.0 Å, respectively. The structures reveal the amino acid residues critical for stabilization of the tetrameric assembly and for the exceptionally tight binding of biotin. Each monomer is an eight-stranded antiparallel β-barrel, remarkably similar to that of the genetically distinct bacterial analog streptavidin. As in streptavidin, binding of biotin involves a highly stabilized network of polar and hydrophobic interactions. There are, however, some differences. The presence of additional hydrophobic and hydrophilic groups in the binding site of avidin (which are missing in streptavidin) may account for its higher affinity constant. Two amino acid substitutions are proposed to be responsible for its susceptibility to denaturation relative to streptavidin. Unexpectedly, a residual *N*-acetylglucosamine moiety was detected in the deglycosylated avidin monomer by difference Fourier synthesis.**

The biotin-binding proteins avidin (from egg white) and streptavidin (from the bacterium *Streptomyces avidinii*) occupy a place of honor in many fields of biology. The reason for interest in these proteins is 2-fold: (*i*) both proteins exhibit the highest known affinity ($K_a \approx 10^{15}$ M^{-1}) in nature between a ligand and a protein (1), and (*ii*) largely as a consequence, the avidin–biotin (and streptavidin–biotin) system has been widely applied as a universal tool, particularly for diagnostic purposes (2).

Several groups have tried to crystallize egg-white avidin (3–5) with only limited success. During the course of our studies, which involved chemical and physical properties of avidin, we succeeded in isolating an active deglycosylated form of this protein (6), the structure of which we report here.‡ Interestingly, the x-ray structure of the related, naturally nonglycosylated, bacterial protein streptavidin has already been determined (7, 8). Comparison of these two genetically remote structures permits us to decipher the crucial elements for formation of such a strong binding site. It had been noted (9) that the primary structures of the two proteins are similar (see Fig. 1) and that the conserved amino acid residues are mostly confined to six homologous segments (10, 11). The current study has revealed that the major structural elements are also conserved and critical functional groups are retained in the binding site. Nevertheless, there are some notable differences in their properties, many of which can be explained in terms of the three-dimensional structures of avidin and streptavidin.

MATERIALS AND METHODS

Crystallization and Data Collection. "Lite avidin" (i.e., avidin with most of the oligosaccharide chain removed) was supplied by Belovo Chemicals (Bastogne, Belgium). It was ≈10-fold less soluble than avidin, apparently due to removal of the carbohydrates. Crystals (space group $P2_12_12$; a = 72.22 Å, b = 80.42 Å, c = 43.33 Å, with two avidin monomers in the asymmetric unit) were grown at 19°C in hanging drops, consisting of 5 μl of protein solution (4 mg/ml) and 5 μl from the reservoir, which contained 23% polyethylene glycol 1000 and 20 mM citrate buffer (pH 5.4). Crystallization conditions and cell parameters were similar to those reported for glycosylated avidin (4). For larger crystals, macroseeding techniques were applied (12). Crystals of the avidin–biotin complex were obtained by soaking biotin into crystals of avidin. The cell constants of the avidin–biotin complex (a = 72.15 Å, b = 80.37 Å, c = 43.54 Å) differ only slightly from those of the native protein. X-ray diffraction data were collected at room temperature on a Siemens/Xentronics multiwire area detector and processed by using the XDS data reduction program (13).

Structure Determination. Our starting model for the lite avidin–biotin complex was a partially refined structure of avidin (kindly provided by W. Hendrickson, Howard Hughes Medical Institute, Columbia University), which had been determined by molecular replacement using streptavidin as a search model (7) and then refined to R = 0.257 at a resolution range of 6–3.2 Å (A. Pähler and W. A. Hendrickson, personal communication). After initial rigid body refinement (14, 15), the R factor for the avidin–biotin complex was 0.45 for 8.0–3.0 Å resolution. Our attempts to refine the structure using X-PLOR (15–17) failed to reduce the R factor below 0.28; the $2F_{obs} - F_{calc}$ electron density maps were discontinuous in some of the loop regions. When examining the fit of the avidin amino acid sequence to the maps, it was clear that one of the strands (β4; Fig. 1) was four residues out of register; Lys-45 pointed toward a number of hydrophobic residues, and the electron density near Ser-47 appeared too short for such a residue. To resolve this inconsistency in this region, we shifted the sequence four residues relative to the electron density map (Fig. 2), resulting in Lys-45 being replaced by Leu-49 and in Ser-47 being replaced by Gly-51. Although these changes allowed us to fit this part of the molecule better into the map, most of the loop regions still lacked clear electron density, and the structure could not be refined to a significantly lower R factor. We were able to overcome this problem by the use of noncrystallographic symmetry averaging of the electron density maps (refs. 18–20; unpublished results). We applied map averaging and solvent flattening, starting from the initial model phases and then extending the phases from 4 to 3 Å resolution by using the DEMON program suite (F. M. D. Vellieux, personal communication). The final averaged map was significantly improved, enabling us to trace the various regions of the molecule that could not be determined previously.

Following these two crucial steps that removed the initial model bias—i.e., the four-residue shift and the use of real-

The publication costs of this article were defrayed in part by page charge payment. This article must therefore be hereby marked "*advertisement*" in accordance with 18 U.S.C. §1734 solely to indicate this fact.

‡The atomic coordinates and structure factors have been deposited in the Protein Data Bank, Chemistry Department, Brookhaven National Laboratory, Upton NY 11973 (reference 1AVI).

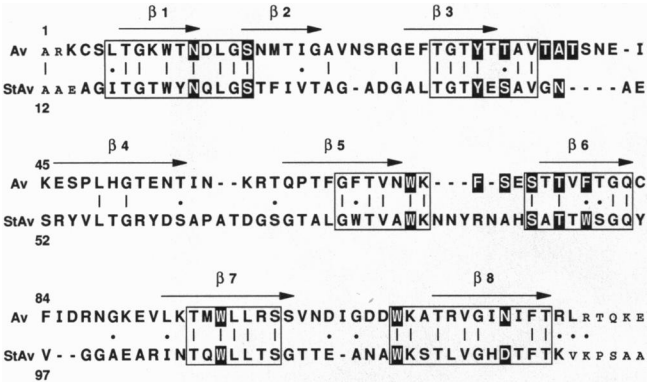

FIG. 1. Alignment of primary structures of avidin (Av) and streptavidin (StAv) based on the three-dimensional spatial position of the individual amino acids in the corresponding structures. N- and C-terminal residues, shown in smaller typeface, are part of the sequence but were not seen in the x-ray structures. Conserved residues are denoted by vertical lines. Similar residues (A, G; S, T; D, E; V, L, I, M; F, W, Y) are indicated by dots. The six homologous segments are enclosed in boxes. Positions of the respective β-strands are marked by arrows. Residues in the binding site, of both proteins, that interact directly with biotin are shown in white type. For each protein, the position of the initial residue in each line is shown on the left of each row. The overall homology in the alignment of the two sequences is 30% identity (41% similarity); the respective values are 64% (74%) within the homologous segments and 7% (17%) outside of these segments.

space noncrystallographic symmetry map averaging—the avidin–biotin complex was fitted into the electron density map by using the program FRODO (21, 22). It was refined with X-PLOR (15–17) by using the simulated annealing slow-cooling protocol with tight noncrystallographic symmetry restraints between monomers (see Table 1). Solvent molecules were gradually added during the refinement process. No electron density was seen for the N and C termini of the molecule; thus, it was possible to build and refine only residues 3–123. All the residues are within allowed regions of the Ramachandran plot. The structure of biotin-free avidin was solved based on the refined structure of the avidin–biotin complex. The biotin and water molecules were removed prior to refinement. Initial rigid body refinement was applied, followed by positional refinement with X-PLOR. Solvent molecules were added at various refinement stages. In the course of the model building, we observed that one of the loops (residues 36–44 between strands β3 and β4) had no density and concluded that this region is disordered in the biotin-free avidin structure. Except for this loop, there is little difference in structural features between avidin and the avidin–biotin complex; the rms deviation was 0.42 Å between 112 pairs of equivalent C^{α} s. All the residues of the avidin structure are within allowed regions of the Ramachandran plot. The refinement results are shown in Table 1.

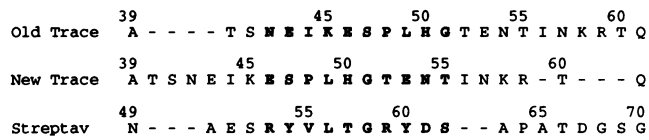

FIG. 2. Schematic of the four-residue shift in the avidin model. Aligned sequences of the initial model (Old Trace) and the new model after the shift (New Trace) are compared to the streptavidin sequence (Streptav). Residues that are part of β4 are indicated in boldface type. This four-residue shift causes the loop between strands β4 and β5 to become smaller, whereas the loop between strands β3 and β4 becomes larger.

Table 1. Refinement results for avidin–biotin complex and avidin structures

	Avidin–biotin	Avidin
Program used	X-PLOR	X-PLOR
R factor	15.1%	18.8%
Resolution range	8.0–3.0 Å	8.0–2.6 Å
No. of observed reflections	4984*	7519*
Completeness of data	98.5%	95.0%
Final model		
2 avidin monomers	1892 atoms	1768 atoms
2 biotin molecules	32 atoms	—
2 GlcNac	28 atoms	28 atoms
Waters	74 molecules	103 molecules
Protein $\langle B_{iso} \rangle$	11.3 Å^2	15.9 Å^2
Biotin $\langle B_{iso} \rangle$	7.3 Å^2	—
GlcNac $\langle B_{iso} \rangle$	20.3 Å^2	27.7 Å^2
Waters $\langle B_{iso} \rangle$	23.9 Å^2	24.9 Å^2
rms deviations from ideality		
Bond length	0.013 Å	0.013 Å
Bond angle	1.83°	1.84°
rms deviation of C^{α} between noncrystallographic symmetry-related monomers	0.26 Å	0.31 Å

*All $F_{obs} > 0$ were included in refinement.

RESULTS

The overall fold of the avidin monomer closely resembles that of streptavidin; it is constructed of eight antiparallel β-strands (Figs. 1 and 3), which form a classical β-barrel. The most striking differences in their tertiary fold lie in the size and conformation of the six extended loops that connect the strands.

There are three regions of monomer–monomer interaction in avidin (Fig. 4). These interactions contribute to the rigidity of the quaternary structure and also provide part of the framework for the tight binding of biotin. Comparison of

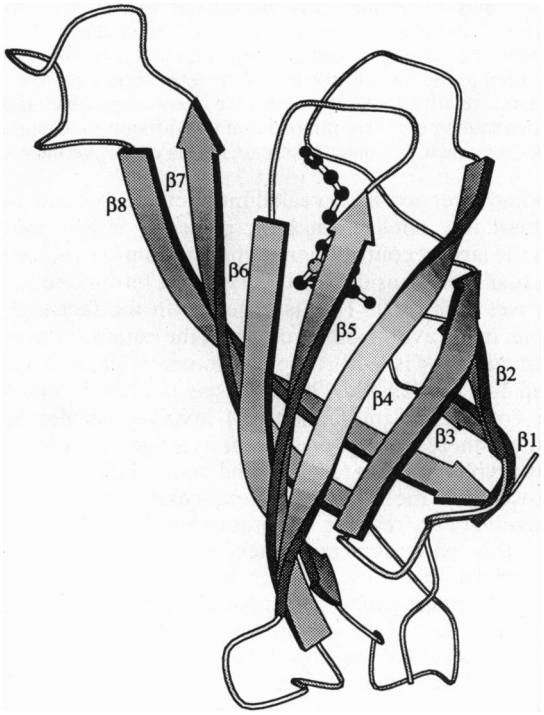

FIG. 3. A MOLSCRIPT ribbon diagram (31) of the avidin–biotin monomer, with the eight strands of the β-barrel labeled. Biotin molecule is shown in a ball and stick model.

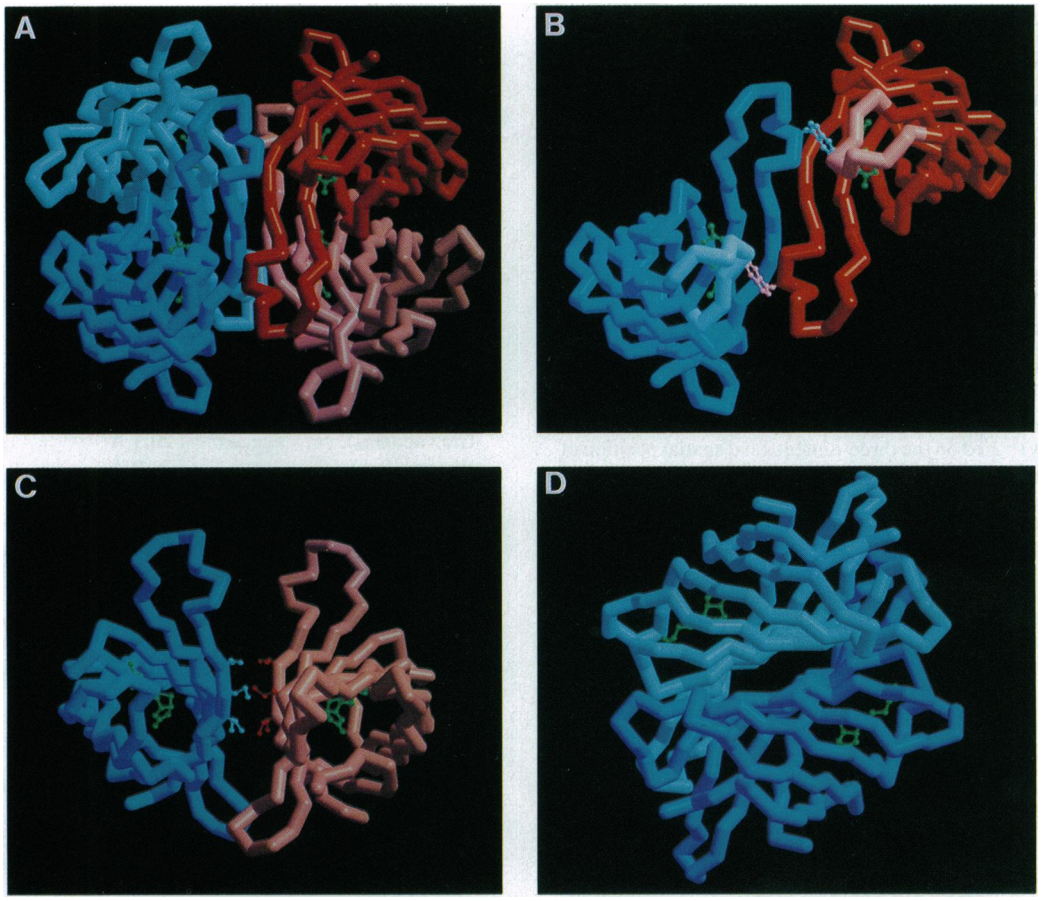

FIG. 4. Quaternary structure of avidin, drawn using RASTER3D (32). (*A*) Quaternary structure of the avidin tetramer. The four bound biotin molecules are shown in green in this and subsequent panels. Colors of the monomer are enumerated as follows: 1, blue; 2, red; 3, pink; 4, powder blue. (*B*) Interaction 1–2 occurs between monomers 1 and 2, which are related by a crystallographic two-fold axis. Monomers are linked by hydrogen-bond interactions between the respective N-terminal portions of the β8-strands of each monomer, which, in consequence, form a short antiparallel β-sheet. Notably, as a result of this interaction, each monomer contributes Trp-110 (shown in pastel colors) to its partner as an additional and very significant component of the biotin-binding site. When biotin is bound, interaction 1–2 is enhanced greatly, owing to the Trp-110–biotin interaction. Loop denoted in a pastel color (residues 36–44) folds into a defined structure only upon binding of biotin. (*C*) Interaction 1–3, between monomers 1 and 3 (rotated slightly about the vertical axis compared to *A*), is relatively weak, involving only three equivalent hydrophobic residues from each monomer—i.e., Met-96, Val-115, and Ile-117. Resultant van der Waals interactions have the least contribution to the overall stability of the tetrameric structure of avidin. (*D*) Interaction 1–4, between monomers 1 and 4 (rotated 90° about the vertical axis relative to *A*), is an intricate interaction, which is decisive to the observed structural stability of the avidin tetramer. The cohesion of the two monomers is so intimate that it is difficult to distinguish between them in the resultant dimer. Sections of four β-strands (β4, β5, β6, and β7) from each monomer take part in this extensive interaction.

avidin and streptavidin revealed interactions 1–2 and 1–4 to be remarkably similar. In both proteins, interaction 1–4 makes the largest contribution to the tetrameric structure and can actually be considered to serve as a tetrameric glue in both cases (Fig. 4*D*). This is reflected in the fact that, for example, in the avidin–biotin complex the buried surface area of interaction 1–4 is 1951 Å^2 per monomer, while interactions 1–2 and 1–3 are 729 and 120 Å^2, respectively (15, 24). Most of the contacts in interaction 1–4 involve van der Waals forces, but there are also prominent hydrogen-bonding interactions involving polar residues and water molecules. There are, however, some intriguing differences between avidin and streptavidin with respect to interaction 1–3 (Fig. 4*C*). In avidin, this particular monomer–monomer interaction is characterized solely by van der Waals forces, whereas in streptavidin polar amino acid residues predominate. Thus, Met-96 and Ile-117 in avidin are replaced in the three-dimensional structure by Gln-107 and His-127 in streptavidin, while Val-115 in avidin is conserved in streptavidin (Val-125). Consequently, instead of the homologous hydrophobic interactions in avidin (formed between Met-96 and Ile-117 and their equivalent residues on the opposing monomers), the side chain of Gln-107 in streptavidin forms a hydrogen bond with the main-chain oxygen of the opposing Val-125, while the equivalent histidines of the two monomers stack one on top of the other.

The biotin-binding site is positioned near one end of the avidin barrel (Fig. 3). It contains an array of polar and aromatic residues, all of which are involved in the tight binding. The binding site residues appear to be exquisitely positioned to provide a precise fit to biotin. In fact, in the unoccupied binding site, the structure of the bound solvent molecules bears resemblance to the shape of the biotin molecule (data not shown), reminiscent, for example, of the water structure in the binding pocket of protease A from *Streptomyces griseus*, which also seems to emulate the shape of the substrate (24). During the course of binding, biotin replaces the network of solvent molecules, and one of the exposed loops [residues 36–44; i.e., the loop that connects β3 to β4 (Fig. 4)] becomes ordered and locks the biotin in the binding site. In the process, three amino acid residues in the loop contribute additional interactions with the biotin molecule (Fig. 4*B*).

Several aromatic residues in the biotin-binding site form a "hydrophobic box" in which the biotin molecule resides (Fig. 5*A*). Two tryptophans, Trp-70 and Trp-97, are anchored by hydrogen bonding to other residues, thus stabilizing the

binding site. One difference between the binding pockets of avidin and streptavidin is the substitution of Trp-92 in streptavidin for Phe-79 in avidin; the second difference is the existence of an additional aromatic residue in avidin, Phe-72, which does not have a streptavidin equivalent. Thus, in streptavidin, only four aromatic residues (all tryptophans) participate in the binding of biotin.

In addition to the hydrophobic interactions described above, the heteroatoms in the ureido ring of biotin exhibit five crucial hydrogen-bond interactions with the side chains of polar amino acid residues (Fig. 5 *C* and *D*). In streptavidin, the biotin-binding site shares a very similar set of features in terms of the hydrogen-bonding network with the biotin rings, the only exceptions being the respective substitutions of Ser-45 and Asp-128 in the bacterial protein for Thr-35 and Asn-118 in avidin (Fig. 1).

The valeryl carboxylate moiety of biotin is involved in five hydrogen-bonding interactions with avidin (Fig. 5*C*). The equivalent interaction in streptavidin is weaker (Fig. 5*D*), since each oxygen forms only one hydrogen bond.

DISCUSSION

Knowledge of the three-dimensional structures of both avidin and streptavidin allows us to compare their binding properties at the atomic level. Both proteins have a conserved tyrosine-containing stretch [homologous segment II (Fig. 1)], consisting of eight amino acid residues, in which the tyrosine (Tyr-33 in avidin, Tyr-43 in streptavidin) occupies an identical spatial position in the two proteins and forms a critical hydrogen bond with the ureido oxygen group of biotin. The crystallographic data are in full agreement with chemical modification data obtained in solution, which demonstrated the essentiality of the hydroxyl group of this particular tyrosine (25, 30). The interaction of this tyrosine with biotin may, in fact, be definitive, as suggested by the isolation and synthesis of minimized biotin-binding fragments of avidin (26), which encompass the tyrosine-containing segment.

The x-ray data show the presence of tryptophan residues in the biotin-binding site of both avidin (residues 70, 97, and 110) and streptavidin (residues 79, 92, 108, and 120). Again, these data are in good agreement with chemical modification data. Thus, modification of tryptophans with 2-hydroxy-5-nitrobenzyl bromide results in the loss of biotin binding (27, 28). Furthermore, the avidin–biotin complex is not modified by the same reagent. Interestingly, of the tryptophan residues in the binding pocket, only one (Trp-70 in avidin and Trp-79 in streptavidin) is not modified by 2-hydroxy-5-nitrobenzyl bromide. This is somewhat surprising, since it appears to be the most accessible tryptophan residue in the pocket (Fig. 5). It therefore seems that the modifying reagent first penetrates deep within the unoccupied binding site and displaces at least part of the bound solvent molecules therein. The reagent thus occupies the position that anticipates the biotin bicyclic ring system, its reactive bromide group being oriented toward the less accessible tryptophan residues. In any case, the x-ray structures of both proteins show that none of the tryptophans are contact residues but are involved in construction of the hydrophobic box, which lures the biotin molecule. This result seems to contradict one of the principles of chemical modification; hence, it is not necessary to modify a contact residue to lose activity, but destruction of an essential structural element is sufficient to do so. Indeed, this serves as an example of chemical modification studies giving equivocal or misleading results, which can only be clarified by solving the structure of the protein.

There are only two major differences between the binding sites of avidin and streptavidin. The first is an additional

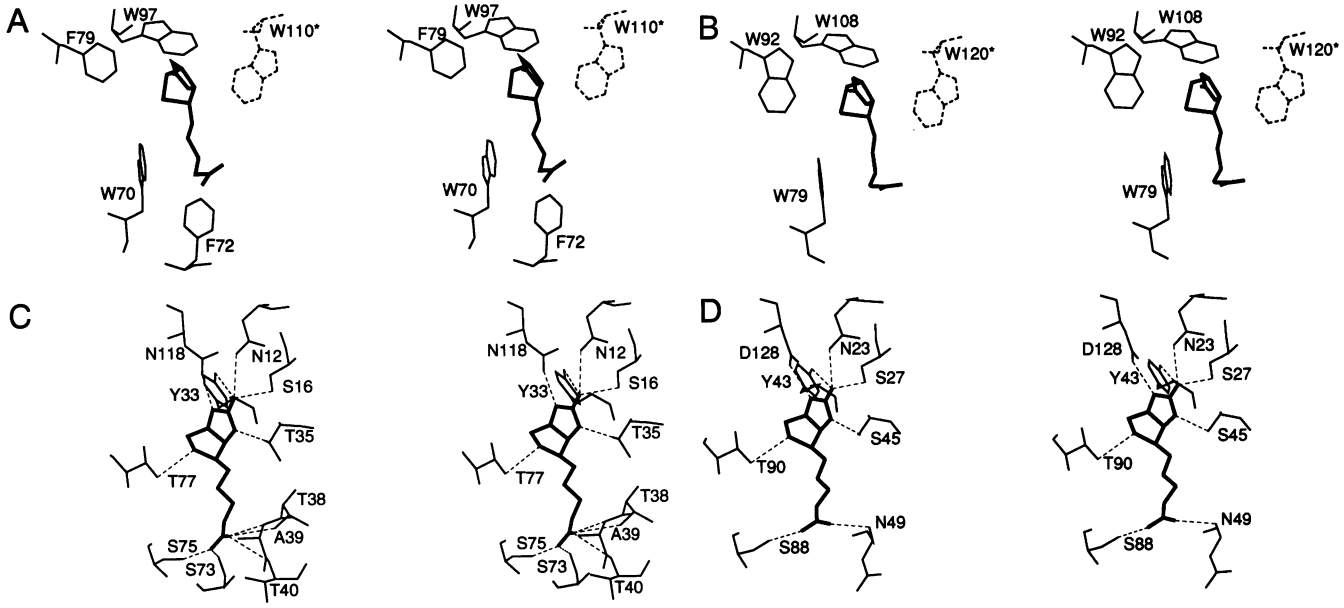

FIG. 5. Binding sites of avidin and streptavidin (streptavidin–selenobiotin coordinates were provided by W. A. Hendrickson). (*A*) Hydrophobic residues in the binding site of avidin. These include Trp-70, Phe-72, Phe-79, and Trp-97 from one monomer, and Trp-110 (dashed lines), which is provided by the adjacent symmetry-related monomer. (*B*) Hydrophobic residues in the binding site of streptavidin. Trp-79, Trp-92, and Trp-108 from one monomer, and Trp-120 (dashed lines) from the adjacent monomer are shown. (*C*) Hydrophilic interactions in the binding site of avidin. Ureido oxygen of the biotin molecule forms three hydrogen bonds with the side chains of Asn-12, Ser-16, and Tyr-33 of avidin forming a tetrahedral oxyanion. In addition, each of the two ureido nitrogens participates in a single hydrogen-bond interaction with Thr-35 and Asn-118. The biotin sulfur may interact with Thr-77. The two carboxylate oxygens of the valeryl moiety of biotin form five hydrogen bonds. One interacts with the main chain N···H of Ala-39 and Thr-40 as well as the side chain of Thr-38 (these residues are part of the loop that is stabilized when biotin is bound), and the other forms hydrogen bonds with the side chains of Ser-73 and Ser-75. (*D*) Hydrophilic interactions in the binding site of streptavidin. In streptavidin, a network of hydrogen bonds, similar to that in the binding site of avidin, is formed with the biotin rings. Ureido ring oxygen forms three hydrogen bonds with Asn-23, Ser-27, and Tyr-43. Each of the ring nitrogens forms one hydrogen bond with Ser-45 and Asp-128, and the biotin sulfur may form a hydrogen bond with Thr-90. Carboxylate oxygens of the biotin valeryl moiety form a total of only two hydrogen bonds—i.e., one with the main chain N···H of Asn-49 (substituted for Ala-39 in avidin) and the other with Ser-88 (the equivalent of Ser-75 in avidin).

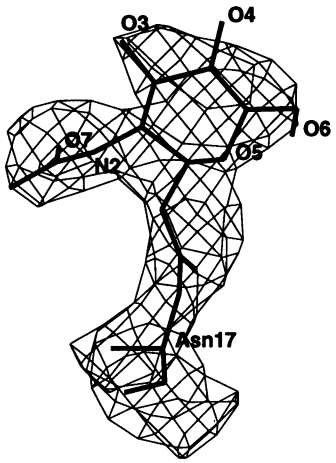

FIG. 6. Electron density map of the single glycosylation site in the avidin monomer; $2F_{obs} - F_{calc}$ electron density is shown around Asn-17 with no sugar included in the refinement at this stage. The unexpected additional density shown could be fit very well with the GlcNAc sugar. Map is contoured at 0.8σ above the mean density level. Noncarbon atoms of GlcNAc are labeled.

aromatic group (Phe-72) in the avidin binding pocket—i.e., it contains five aromatic residues whereas the streptavidin pocket contains only four. The x-ray structure of the avidin–biotin complex shows that Phe-72 interacts with the valeryl side chain of biotin. The second major difference is in the hydrogen-bonding network with the valeryl carboxylate group. In streptavidin, the biotin carboxylate forms only two hydrogen bonds, whereas in avidin there are five. These two factors—an additional aromatic residue and three more hydrogen bonds—may help explain why the binding of biotin to avidin is reportedly tighter than that to streptavidin [$K_d = 6 \times 10^{-16}$ versus 4×10^{-14} M, respectively (29)].

Another difference between avidin and streptavidin may also contribute to their different affinities for biotin. The lengths of the loops that become ordered upon binding of biotin (residues 36–44 in avidin and 45–50 in streptavidin) are significantly different. The longer loop of avidin provides tighter closure of the occupied binding site.

As already noted, avidin contains a single glycosylation site, which is lacking in the bacterial streptavidin. For crystallization, we chose to use a deglycosylated form of avidin, which had been assumed to be totally devoid of sugar, based on interaction with lectins and total sugar analysis (6). It was thus surprising to discover (on the basis of difference Fourier synthesis) that the proximal sugar residue (i.e., *N*-acetylglucosamine) remained intact (Fig. 6), providing an example of the presence of a sugar residue on a protein being detected by crystallographic methods after chemical and biochemical analyses failed to do so.

It remains a puzzle why nature has produced such specific and similar biotin-binding proteins in both eukaryotes and prokaryotes. The function(s) of these proteins in nature also remains a puzzle since, in fact, it is still unknown whether biotin is the sole, the primary, or even the genuine ligand for either protein. It seems unreasonable, however, to assume that the similarity of avidin and streptavidin and their remarkable biotin-binding properties are merely the result of an evolutionary fluke.

Note Added in Proof. Recently, a tetragonal form of avidin was determined (33).

We thank W. A. Hendrickson and A. Pähler for kindly providing the avidin and streptavidin–selenobiotin structures and F. R. Salemme and P. C. Weber for supplying the streptavidin–biotin structure; F. Frolow for help in data collection and valuable discussion; C. Oefner for assistance in detecting the four-residue shift in the chain tracing; F. M. D. Vellieux for great assistance in the map averaging procedure; Y. Hiller for isolating the initial preparations of "nonglycosylated" avidin; and I. Silman and P. Axelsen for their comments on the manuscript. This work was supported by the Kimmelman Center (Rehovot, Israel) and the Fund for Basic Research (Israel Academy of Sciences and Humanities).

1. Green, N. M. (1975) *Adv. Protein Chem.* **29**, 85–133.
2. Wilchek, M. & Bayer, E. A. (1988) *Anal. Biochem.* **171**, 1–32.
3. Green, N. M. & Joynson, M. A. (1970) *Biochem. J.* **118**, 71–72.
4. Pinn, E., Pähler, A., Saenger, W., Petsko, G. A. & Green, N. M. (1982) *Eur. J. Biochem.* **123**, 545–546.
5. Gatti, G., Bolognesi, M., Coda, A., Chiolerio, F., Filippini, E. & Malcovati, M. (1984) *J. Mol. Biol.* **178**, 787–789.
6. Hiller, Y., Gershoni, J. M., Bayer, E. A. & Wilchek, M. (1987) *Biochem. J.* **248**, 167–171.
7. Hendrickson, W. A., Pähler, A., Smith, J. L., Satow, Y., Merritt, E. A. & Phizackerley, R. P. (1989) *Proc. Natl. Acad. Sci. USA* **86**, 2190–2194.
8. Weber, P. C., Ohlendorf, D. H., Wendoloski, J. J. & Salemme, F. R. (1989) *Science* **243**, 85–88.
9. Argaraña, C. E., Kuntz, I. D., Birken, S., Axel, R. & Cantor, C. R. (1986) *Nucleic Acids Res.* **14**, 1871–1882.
10. Wilchek, M. & Bayer, E. A. (1989) *Trends Biochem. Sci.* **14**, 408–412.
11. Bayer, E. A. & Wilchek, M. (1990) *J. Chromatogr.* **510**, 3–11.
12. Thaller, C., Eichele, G., Weaver, L. H., Wilson, E., Karlsson, R. & Jansonius, J. N. (1985) *Methods Enzymol.* **114**, 132–135.
13. Kabsch, W. (1988) *J. Appl. Crystallogr.* **21**, 916–924.
14. Sussman, J. L., Holbrook, S. R., Church, G. M. & Kim, S.-H. (1977) *Acta Crystallogr. A* **33**, 800–804.
15. Brünger, A. T. (1992) *X-PLOR 3.0* (Yale Univ., New Haven, CT).
16. Brünger, A. T., Kuriyan, J. & Karplus, M. (1987) *Science* **235**, 458–460.
17. Brünger, A. T., Krukowski, A. & Erickson, J. W. (1990) *Acta Crystallogr. A* **46**, 585–593.
18. Argos, P., Ford, G. C. & Rossmann, M. G. (1975) *Acta Crystallogr. A* **31**, 499–506.
19. Piontek, K., Chakrabarti, P., Schär, H. P., Rossmann, M. G. & Zuber, H. (1990) *Proteins* **7**, 74–92.
20. Rossmann, M. G., McKenna, R., Tong, L., Xia, D., Dai, J.-B., Wu, H., Choi, H.-K. & Lynch, R. E. (1992) *J. Appl. Crystallogr.* **25**, 166–180.
21. Jones, T. A. (1978) *J. Appl. Crystallogr.* **11**, 268–272.
22. Pflugrath, J. W., Saper, M. A. & Quiocho, F. A. (1984) in *Methods and Applications in Crystallographic Computing*, eds. Hall, S. & Ashiaka, T. (Clarendon, Oxford, U.K.), pp. 404–407.
23. Lee, B. & Richards, F. M. (1971) *J. Mol. Biol.* **55**, 379–400.
24. James, M. N. G., Sielecki, A. R., Brayer, G. D., Delbaere, L. T. J. & Bauer, C. A. (1981) in *Structural Aspects of Recognition and Assembly in Biological Macromolecules*, eds. Balaban, M., Sussman, J. L., Traub, W. & Yonath, A. (Balaban ISS, Rehovot, Israel), pp. 3–18.
25. Wynne, D., Wilchek, M. & Novogrodsky, A. (1976) *Biochem. Biophys. Res. Commun.* **68**, 730–739.
26. Hiller, Y., Bayer, E. A. & Wilchek, M. (1991) *Biochem. J.* **278**, 573–585.
27. Gitlin, G., Bayer, E. A. & Wilchek, M. (1988) *Biochem. J.* **250**, 291–294.
28. Gitlin, G., Bayer, E. A. & Wilchek, M. (1988) *Biochem. J.* **256**, 279–282.
29. Green, N. M. (1990) *Methods Enzymol.* **184**, 51–67.
30. Gitlin, G., Bayer, E. A. & Wilchek, M. (1990) *Biochem. J.* **269**, 527–530.
31. Kraulis, P. J. (1991) *J. Appl. Crystallogr.* **24**, 946–950.
32. Bacon, D. J. & Anderson, W. F. (1988) *J. Mol. Graph.* **6**, 219–220.
33. Pugliese, L, Coda, A., Malcovati, M. & Bolognesi, M. (1993) *J. Mol. Biol.*, in press.